



Ferrimagnetic cagelike Fe_4O_6 cluster: Structure determination from infrared dissociation spectroscopy

A. Kirilyuk,¹ A. Fielicke,² K. Demyk,^{3,4} G. von Helden,² G. Meijer,² and Th. Rasing¹

¹Radboud University Nijmegen, Institute for Molecules and Materials, NL-6525 AJ Nijmegen, The Netherlands

²Fritz-Haber-Institut der Max-Planck-Gesellschaft, Faradayweg 4-6, D-14195 Berlin, Germany

³Centre d'Étude Spatiale des Rayonnements, Université de Toulouse, F-31028 Toulouse Cedex 4, France

⁴CNRS, UMR 5187, 9 avenue du Colonel Roche, F-31028 Toulouse Cedex 4, France

(Received 14 May 2010; published 19 July 2010)

Cationic iron-oxide clusters of several sizes and stoichiometries have been synthesized and studied isolated in the gas phase. Vibrational spectra of the clusters have been measured using resonant IR-induced dissociation of $\text{Fe}_n\text{O}_{m+2}^+ \rightarrow \text{Fe}_n\text{O}_m^+ + \text{O}_2$ in the 250–1250 cm^{-1} range. Density-functional theory was used to investigate the geometry and spin configuration of the representative $\text{Fe}_4\text{O}_6^{0/+}$ cluster. Its lowest-energy state was found to be an almost tetrahedral cagelike structure with a ferrimagnetic arrangement of spins, resulting in total cluster spin of $S=5$ for the neutral cluster. These results were confirmed for Fe_4O_6^+ by the comparison of the calculated infrared spectrum to the experimentally obtained one.

DOI: [10.1103/PhysRevB.82.020405](https://doi.org/10.1103/PhysRevB.82.020405)

PACS number(s): 36.40.Cg, 36.40.Mr, 61.46.Bc, 73.22.-f

With the continuous trend of increasing the density of electronic devices, novel concepts are needed to answer the increasing technical problems. Many of these concepts require the creation of dedicated nanosized building blocks with well understood and *a priori* designed properties. For application in quantum computing and storage, for example, chemically synthesized magnetic molecules were suggested as possible units.¹

In such a “bottom-up” approach, magnetic clusters represent the smallest chunks of matter where condensed matter properties start to appear, magnetic order, in particular. However, these properties are still drastically different from those of the bulk matter, making the clusters a new object of physical research. Such atomic clusters may be as small as containing only tens of atoms.² They allow a large freedom in manipulation through varying their composition and size, adding one atom at a time.³ From various materials, transition-metal oxides represent the widest variety of phenomena, from ferroelectricity and magnetism to superconductivity, often combined. In cluster form, many unusual phenomena have been predicted.^{4–8} The knowledge of their detailed magnetic, electronic, and ionic structure is essential for various applications, such as the formation of novel materials or design of next generation devices, to fundamental issues as the functioning of quantum and thermodynamics laws in (sub-) nanoscale systems.

To explore the intrinsic properties of nanoparticles free of external perturbations, experiments are best performed in the gas phase. However, the experimental data on the properties of gas-phase transition-metal oxide clusters are still scarce. A preferred method to obtain information on structure and bonding is vibrational spectroscopy. Unfortunately, in most cases, isolated clusters can only be studied in molecular beams or ion traps⁹ and the low particle density rules out direct absorption measurements. Furthermore, clusters are often produced in broad size distributions, making size selectivity essential. To overcome such problems, mass selected clusters can be embedded and accumulated in rare gas matrices.^{10,11} In those experiments, interactions with the rare

gas matrix may induce shifts of the absorption lines, and additionally, it cannot be excluded that structural changes during the deposition occur. Intense tunable infrared sources such as free-electron lasers allow different approaches. Thus, titanium¹² and zirconium¹³ oxides were investigated with the help of infrared resonance enhanced multiple-photon ionization spectroscopy. Infrared photodissociation spectroscopy helped to determine the structure of oxide clusters of vanadium,¹⁴ niobium and tantalum^{15,16} as well as binary vanadium-titanium oxide clusters.¹⁷ However, the possible existence of magnetic order has not been investigated for either of these systems.

Here we report an experimental investigation of cationic iron-oxide clusters in the gas phase. Their vibrational spectra are measured via resonant dissociation of the target clusters (Fe_nO_m^+) tagged with molecular oxygen. Quantum chemical calculations allow us to derive the cluster structure as well as its magnetic state by comparison of the calculated vibrational spectra for low-energy isomers to the experimental data. A ferrimagnetic structure slightly distorted from C_{3v} symmetry is found for a “bulk-stoichiometric” Fe_4O_6^+ cation cluster while the lowest-energy neutral Fe_4O_6 isomer is of exact C_{3v} symmetry. The calculations also demonstrate a correlation between the cluster’s geometrical and magnetic configurations.

The cluster cations are produced by ablating the metal with the second harmonic output (532 nm, 10 mJ) of a pulsed Nd-yttrium aluminum garnet laser and quenching the plasma with a short pulse of a gas mixture containing 0.5% oxygen in helium. After expansion into vacuum the cluster distribution in the molecular beam is analyzed using a reflectron time-of-flight mass spectrometer. The cluster beam is overlapped with a counterpropagating intense infrared laser beam, delivered by the free electron laser for infrared experiments (FELIX). This laser can produce intense several μs long pulses of tunable IR radiation in the 40–2500 cm^{-1} range containing up to 100 mJ per pulse. Each pulse consists of a train of 0.3–3 ps long micropulses of typically 10 μJ , spaced by 1 ns. For more details of the measurement procedure see Ref. 16.

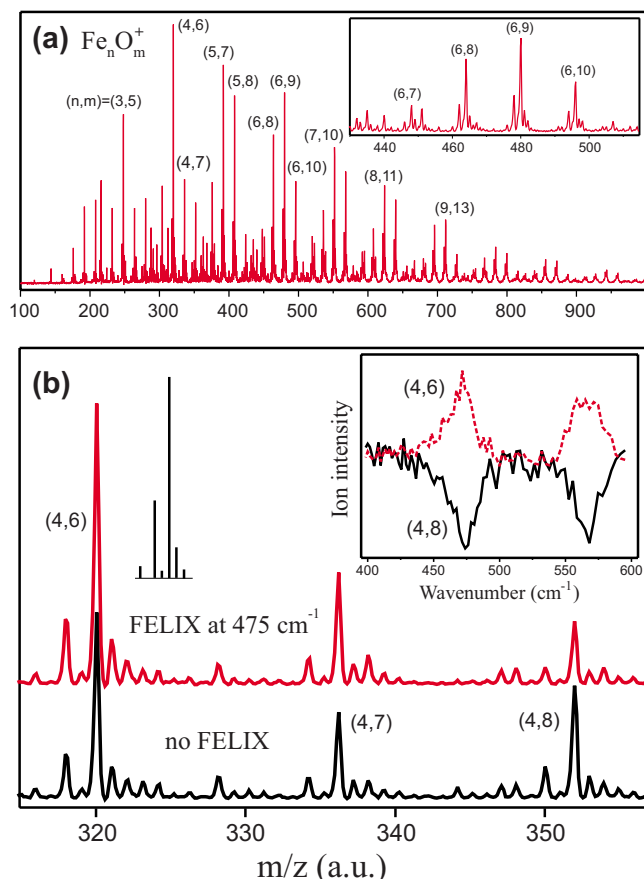


FIG. 1. (Color online) (a) An example mass spectrum of Fe_nO_m^+ ions. (b) Part of the mass spectrum of Fe_nO_m^+ ions illustrating its change under the influence of the IR laser radiation. The structure of the mass peaks is due to the natural isotope distribution of iron, which is illustrated by the calculated isotope pattern of Fe_4O_6^+ . The inset shows the dependence of the peak intensities on the FELIX frequency.

A typical mass spectrum of the cationic iron-oxide cluster distribution is shown in Fig. 1(a). The cluster-formation conditions are optimized to yield small clusters with less than 10–12 iron atoms in high intensity. The distribution mainly contains iron-oxide clusters with an Fe/O ratio of 1.2–1.9, that corresponds to a formal oxidation state of iron between +2 and +4. On average, this is close to the values for both the stoichiometric hematite Fe_2O_3 as well as for the magnetite Fe_3O_4 .

In the gas phase, the absorption of photons can be detected by monitoring the dissociation of weakly bound cluster complexes. Monitoring the dissociation yield as a function of photon energy then gives the absorption spectrum. Indeed, if the laser light is resonant with an IR-active mode of a cluster, one or more photons can be absorbed by the cluster. If this leads to dissociation, the corresponding mass spectrometric intensity will be decreased [see Fig. 1(b)]. IR multiple photon dissociation (IR-MPD) spectra are constructed by recording the ion intensities of the clusters, both parents and products, as a function of the FELIX frequency [see inset in Fig. 1(b)]. The use of mass spectrometric detection of the IR-induced dissociation allows for cluster size

specific measurement of the IR absorption spectra.

As a function of their composition, the iron-oxide clusters show a very different dependence of the dissociation yield on the IR intensity. This allowed us to distinguish between particularly stable clusters, that never showed any dissociation, (even at fluences of up to 5 mJ/cm^2 in a micropulse, corresponding to the fluence of about 30 J/cm^2 in a 5–7 μs long macropulse) and weakly bound complexes that tend to loose O_2 molecules already at fluences of up to hundred times lower, provided the photon energy is in resonance. The result of such a dissociation is always one of those “stable” clusters.

An example of this is shown in Fig. 1(b), where the intensity of the Fe_4O_8^+ cluster decreases at certain FELIX wavelengths while the signal of Fe_4O_6^+ increases at the same wavelengths by the same amount. On the other hand, the Fe_4O_6^+ cluster never showed any dissociation, even at FELIX intensities more than ten times higher (up to 60 mJ per macropulse) than the one used for the data of Fig. 1(b). Thus, such resonant dissociation provides a unique opportunity to determine the stability pattern of oxide clusters.

Loss of molecular oxygen has also been observed after collisional activation for Fe_nO_m^+ clusters if the iron is in an average formal oxidation state larger than +3 (including Fe_4O_6^+) and it has been concluded that these clusters contain dioxo units. However, for clusters containing less oxygen the dominant fragmentation channels may be the release of FeO or FeO_2 units.¹⁸

The vibrational spectra that can be obtained via IR-MPD are a distinct fingerprint of the original (unstable) cluster. Such cluster, however, is nothing else but a weakly bound complex of a smaller stable cluster with an oxygen molecule (O_2), i.e., the oxygen molecule acts as a “messenger” in the IR-MPD process.

Figure 2 shows the frequency dependence of the intensity enhancement for the more stable Fe_nO_m^+ clusters formed by the fragmentation of the parent $\text{Fe}_n\text{O}_{m+2}^+$ cluster. The frequency dependence of the formation mirrors the depletion of the parent cluster, see inset in Fig. 1(b), indicating the loss of O_2 is indeed the dominant fragmentation channel. Note that the spectra become rather similar for the three heaviest clusters of this set. This may be explained by the emerging bulk-like behavior of these clusters. For comparison, the bulk phonon frequencies of magnetite Fe_3O_4 and hematite Fe_2O_3 (Ref. 19) are indicated in the figure. These frequencies are in a range where especially the larger clusters show several bands, however, we observe also bands at higher frequencies.

Note that the composition of these clusters does not exactly match the stoichiometry of the bulk Fe_2O_3 , as suggested recently.^{20,21} Instead, the composition rather follows the Fe_3O_4 pattern, with Fe_3O_4 , Fe_6O_8 , and Fe_9O_{12} clusters present. The increase of the oxygen concentration in the injected gas mixture did result in clusters with higher O_2 content. However, during the IR dissociation, two O_2 molecules would be removed by the resonant excitation, leaving the composition of those stable clusters unchanged.

Some qualitative conclusions about the cluster geometry can be directly derived from these spectra. For example, weakly bound dioxygen groups (O_2^-) normally have their bands near 1150 cm^{-1} , in Fe-OO the stretch vibration of this

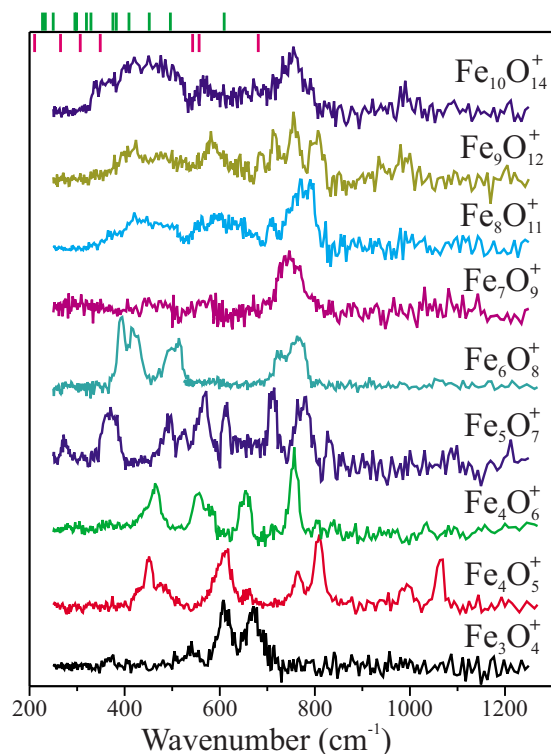


FIG. 2. (Color online) Vibrational spectra of several iron oxide cluster cations obtained via resonant dissociation of the clusters with the excess of oxygen. Cluster compositions are indicated in the figure. For comparison, bulk phonon frequencies of magnetite Fe_3O_4 (below the line) and hematite Fe_2O_3 (above the line) are indicated in the upper part of the figure.

superoxo group is found at 1204 cm^{-1} .²² In none of the clusters bands in this range can be observed, that again indicates the role of O_2 as a physisorbed messenger only, not disturbing the cluster structure. Vibrations of terminal oxygen groups, $\text{Fe}=\text{O}$, are usually observed around 1000 cm^{-1} ; such lines are visible in Fe_4O_5^+ and possibly in the heavy $\text{Fe}_9\text{O}_{12}^+$ and $\text{Fe}_{10}\text{O}_{14}^+$ clusters. At lower frequencies, the vibrations are associated with Fe-O-Fe bridges and other collective excitations.

To obtain more detailed structural information, the experimental spectra can be compared to results from density-functional-theory calculations. This is demonstrated here on the Fe_4O_6^+ cluster. The geometry optimization is performed with the JAGUAR 4.0 (Ref. 23) program using the B3LYP exchange-correlation functional and the LA3CVP* basis set. The harmonic vibrational frequencies and the corresponding IR intensities are computed numerically. The reliability of this method is tested on the smallest clusters (FeO , FeO_2 , and Fe_2O_2) by comparison with existing experimental data as well as calculation results.^{22,24}

First, the structures are optimized for many different Fe_4O_6^+ starting geometries and spin states. The two most stable ones (shown in Fig. 3) are selected for further considerations. For both structures we performed further energy minimizations for a number of fixed spin states of the cluster. No symmetry restrictions are applied at any stage of the calculations. After thorough geometry optimization, the IR

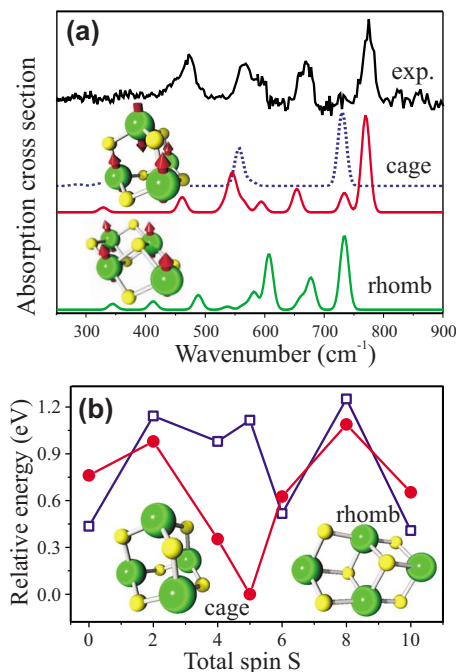


FIG. 3. (Color online) (a) Comparison of the experimental IR spectrum with the calculated IR absorption spectra for the two cationic isomers. The calculated spectra are folded with a Gaussian line-shape function of 10 cm^{-1} full width at half maximum. The dashed curve shows the calculated vibrational spectrum for a neutral Fe_4O_6 cagelike cluster. (b) Relative energy versus spin state for the two low-energy geometries of the neutral Fe_4O_6 cluster.

spectra of the cluster isomers are calculated. Figure 3(a) shows the obtained spectra for the two lowest-energy geometries along with the experimental spectrum for the Fe_4O_6^+ cluster. The spectrum of the cationic cluster in a triangular cage form with total spin $S=9/2$ (ferrimagnetic configuration, that corresponds to the magnetic moments of three Fe atoms “up” and one “down,” minus one spin) fits rather well. For comparison, also the vibrational spectrum of the triangular neutral cluster with the total spin $S=5$ (that is, the nearest spin configuration) is shown. The ionization leads to a small distortion of the original structure, yielding—as a result of the symmetry lowering—a higher number of IR active modes in the cationic cluster. In addition, the vibrational spectrum of the second lowest-energy structure, the cationic rhombic cluster with a total spin of $S=19/2$ (corresponding to the fully ferromagnetic configuration) is also shown. The fit to the experimental data is considerably worse, in particular, the highest-energy band is absent.

The good agreement of the calculated spectrum with experimental data proves the reliability of our theoretical approach. Therefore, we have used it further for more insight into this system and investigated the neutral Fe_4O_6 clusters in the two low-energy geometries of the cations as a function of the total cluster spin. Figure 3(b) shows the obtained results comparing energies of the compact tetrahedron structures with that of the more flat rhombuslike one. The lowest-energy isomer is the tetrahedronlike cage cluster with the total spin $S=5$, resulting from a ferrimagnetic arrangement of the iron magnetic moments: three up, one down. Note that a

similar cage structure, however in a fully ferromagnetic state and therefore with perfect T_d symmetry, was predicted in Ref. 21. Ferrimagnetic arrangement in our case though, explains the slight deviation from a tetrahedral structure leading to C_{3v} symmetry. The equivalent-structure cluster with $S=10$ possesses an exact T_d symmetry but is 0.65 eV higher in energy. The second low-energy geometry has all four iron atoms lying in a plane; its lowest-energy state (+0.40 eV) has ferromagnetic order with $S=10$ and C_{2h} symmetry, the $S=0$ state is nearly isoenergetic.

It is interesting to compare the obtained equilibrium geometry with the bulk structure of Fe_2O_3 . Bulk hematite has a $R\bar{3}c$ space group symmetry and thus belongs to the trigonal class of materials. As such, the obtained triangular structure for the Fe_4O_6 cluster looks like a small chunk of the bulk Fe_2O_3 , however with smaller interatomic distances, 1.81–1.84 Å as compared to 1.95–2.11 Å in bulk Fe_2O_3 .

One should also note the very large magnetic exchange energy of almost 0.1 eV per magnetic atom. This value is tentatively derived from the total energy difference between the two lowest-energy spin configurations that is >0.35 eV. Such energy would mean the Curie temperature of such clusters to be higher than that of the bulk material (~950 K).

This is many times higher than the exchange found in other small magnetic entities—magnetic molecules,^{25,26} even though there are certain similarities with the oxide cores of such materials, in particular, typical ferrimagnetic spin configuration. Therefore such clusters are very interesting for fundamental studies of subnanometer magnetism and may be useful to create new materials with tailored magnetic properties.

To summarize, vibrational spectra of several cationic iron-oxide clusters have been measured with resonant IR dissociation spectroscopy. To obtain the geometric and magnetic structure of the Fe_4O_6^+ model cluster, density-functional-theory calculations have been carried out; the minimum-energy structure explains the experimental vibrational spectrum, confirming a compact, triangular, ferrimagnetic structure for the cation.

This work was supported by Stichting voor Fundamenteel Onderzoek der Materie (FOM) by providing beam time for FELIX. We thank the FELIX staff for their skillful assistance. This work was also supported in part by the EU Initial Training Network FANTOMAS.

¹M. N. Leuenberger and D. Loss, *Nature (London)* **410**, 789 (2001).

²R. F. Service, *Science* **271**, 920 (1996).

³A. W. Castleman, Jr. and S. N. Khanna, *J. Phys. Chem. C* **113**, 2664 (2009).

⁴P. J. Ziemann and A. W. Castleman, Jr., *Phys. Rev. B* **46**, 13480 (1992).

⁵S. K. Nayak and P. Jena, *Phys. Rev. Lett.* **81**, 2970 (1998).

⁶B. V. Reddy and S. N. Khanna, *Phys. Rev. Lett.* **83**, 3170 (1999).

⁷J. Kortus and M. R. Pederson, *Phys. Rev. B* **62**, 5755 (2000).

⁸Q. Sun, M. Sakurai, Q. Wang, J. Z. Yu, G. H. Wang, K. Sumiyama, and Y. Kawazoe, *Phys. Rev. B* **62**, 8500 (2000).

⁹K. R. Asmis, A. Fielicke, G. von Helden, and G. Meijer, in *The Chemical Physics of Solid Surfaces. Atomic Clusters: From Gas Phase to Deposited*, edited by P. Woodruff (Elsevier, Amsterdam, 2007), Vol. 12.

¹⁰K. A. Bosnick *et al.*, *J. Chem. Phys.* **111**, 8867 (1999).

¹¹J. R. Lombardi and B. Davis, *Chem. Rev.* **102**, 2431 (2002); B. Zhao, H. Lu, J. Jules, and J. R. Lombardi, *Chem. Phys. Lett.* **362**, 90 (2002).

¹²K. Demyk, D. van Heijnsbergen, G. von Helden, and G. Meijer, *Astron. Astrophys.* **420**, 547 (2004).

¹³G. von Helden, A. Kirilyuk, D. van Heijnsbergen, B. Sartakov, M. A. Duncan, and G. Meijer, *Chem. Phys.* **262**, 31 (2000).

¹⁴K. R. Asmis and J. Sauer, *Mass Spectrom. Rev.* **26**, 542 (2007).

¹⁵A. Fielicke, G. Meijer, and G. von Helden, *Eur. Phys. J. D* **24**, 69 (2003).

¹⁶A. Fielicke, G. Meijer, and G. von Helden, *J. Am. Chem. Soc.* **125**, 3659 (2003).

¹⁷E. Janssens, G. Santambrogio, M. Brümmer, L. Wöste, P. Lievens, J. Sauer, G. Meijer, and K. R. Asmis, *Phys. Rev. Lett.* **96**, 233401 (2006).

¹⁸D. Schröder, P. Jackson, and H. Schwarz, *Eur. J. Inorg. Chem.* **2000**, 1171 (2000).

¹⁹I. Chamritski and G. Burns, *J. Phys. Chem.* **109**, 4965 (2005).

²⁰S. Yin, W. Xue, X.-L. Ding, W.-G. Wang, S.-G. He, and M.-F. Ge, *Int. J. Mass. Spectrom.* **281**, 72 (2009).

²¹X.-L. Ding, W. Xue, Y.-P. Ma, Z.-C. Wang, and S.-G. He, *J. Chem. Phys.* **130**, 014303 (2009).

²²L. Andrews, G. V. Chertihin, A. Ricca, and Ch. W. Bauschlicher, Jr., *J. Am. Chem. Soc.* **118**, 467 (1996).

²³JAGUAR 4.0; Schrödinger, Inc.: Portland, OR, 1999–2000.

²⁴G. V. Chertihin, W. Saffel, J. T. Yustein, L. Andrews, M. Neurock, A. Ricca, and Ch. W. Bauschlicher, Jr., *J. Phys. Chem.* **100**, 5261 (1996).

²⁵L. Thomas, F. Lioni, R. Ballou, G. Gatteschi, R. Sessoli, and B. Barbara, *Nature (London)* **383**, 145 (1996).

²⁶W. Wernsdorfer, T. Ohm, C. Sangregorio, R. Sessoli, D. Mailly, and C. Paulsen, *Phys. Rev. Lett.* **82**, 3903 (1999).